NAVAL POSTGRADUATE SCHOOL

MONTEREY, CALIFORNIA

THESIS

WAVE OVERTOPPING OF A BARRIER BEACH

by

Natalie A. Laudier

September 2009

Thesis Advisor:	Jamie MacMahan
Second Reader:	Edward B. Thornton

Approved for public release; distribution is unlimited

REPORT DOCUMENTATION PAGE			*Form Approved OMB No. 0704-0188*
Public reporting burden for this collection of information is estimated to average 1 hour per response, including the time for reviewing instruction, searching existing data sources, gathering and maintaining the data needed, and completing and reviewing the collection of information. Send comments regarding this burden estimate or any other aspect of this collection of information, including suggestions for reducing this burden, to Washington headquarters Services, Directorate for Information Operations and Reports, 1215 Jefferson Davis Highway, Suite 1204, Arlington, VA 22202-4302, and to the Office of Management and Budget, Paperwork Reduction Project (0704-0188) Washington DC 20503.			
1. AGENCY USE ONLY ***(Leave blank)***	**2. REPORT DATE** September 2009	**3. REPORT TYPE AND DATES COVERED** Master's Thesis	
4. TITLE AND SUBTITLE Wave Overtopping of a Barrier Beach		**5. FUNDING NUMBERS**	
6. AUTHOR(S) Natalie A. Laudier			
7. PERFORMING ORGANIZATION NAME(S) AND ADDRESS(ES) Naval Postgraduate School Monterey, CA 93943-5000		**8. PERFORMING ORGANIZATION REPORT NUMBER**	
9. SPONSORING /MONITORING AGENCY NAME(S) AND ADDRESS(ES) N/A		**10. SPONSORING/MONITORING AGENCY REPORT NUMBER**	
11. SUPPLEMENTARY NOTES The views expressed in this thesis are those of the author and do not reflect the official policy or position of the Department of Defense or the U.S. Government.			
12a. DISTRIBUTION / AVAILABILITY STATEMENT Approved for public release; distribution is unlimited.		**12b. DISTRIBUTION CODE**	

13. ABSTRACT (maximum 200 words)

An ephemeral river is a seasonal river that flows into the ocean, forming an inlet at certain times of the year, and the river is blocked by a barrier beach that usually forms a lagoon during the rest of the year. Ephemeral rivers are important for both military and civilian communities because these areas are susceptible to rapid, unpredictable flooding and beach breaching. Wave overtopping of barrier beaches is the first step to modeling beach breaching. Carmel River State Beach, in central California, acts a barrier beach for the Carmel River that flows into the Carmel Lagoon. Lagoon height changes were converted to volume changes by a stage-volume curve, then center differenced and averaged to provide total volume rates of change in the lagoon. The van der Meer and Janssen (VJ), European, and Hedges and Reis (HR) overtopping models were compared. The lagoon volume rate of change was compared to the predicted model rate of change for three different overtopping cases in 2006, 2008, and 2009. The models performed similarly with R^2 values of 0.72–0.86 for narrow banded cases, with an average reduction factor of 0.74.

14. SUBJECT TERMS overtopping, run-up, barrier, natural beach, Carmel River Beach			**15. NUMBER OF PAGES** 61
			16. PRICE CODE
17. SECURITY CLASSIFICATION OF REPORT Unclassified	**18. SECURITY CLASSIFICATION OF THIS PAGE** Unclassified	**19. SECURITY CLASSIFICATION OF ABSTRACT** Unclassified	**20. LIMITATION OF ABSTRACT** UU

NSN 7540-01-280-5500

Standard Form 298 (Rev. 2-89)
Prescribed by ANSI Std. 239-18

THIS PAGE INTENTIONALLY LEFT BLANK

Approved for public release; distribution is unlimited

WAVE OVERTOPPING OF A BARRIER BEACH

Natalie A. Laudier
Lieutenant, United States Navy
B.S., United States Naval Academy, 2003

Submitted in partial fulfillment of the
requirements for the degree of

MASTER OF SCIENCE IN METEOROLOGY AND PHYSICAL OCEANOGRAPHY

from the

NAVAL POSTGRADUATE SCHOOL
September 2009

Author: Natalie A. Laudier

Approved by: Jamie MacMahan
Thesis Advisor

Edward B. Thornton
Second Reader

Jeffrey D. Paduan
Chairman, Department of Oceanography

THIS PAGE INTENTIONALLY LEFT BLANK

ABSTRACT

An ephemeral river is a seasonal river that flows into the ocean, forming an inlet at certain times of the year, and the river is blocked by a barrier beach that usually forms a lagoon during the rest of the year. Ephemeral rivers are important for both military and civilian communities because these areas are susceptible to rapid, unpredictable flooding and beach breaching. Wave overtopping of barrier beaches is the first step to modeling beach breaching. Carmel River State Beach, in central California, acts a barrier beach for the Carmel River that flows into the Carmel Lagoon. Lagoon height changes were converted to volume changes by a stage-volume curve, then center differenced and averaged to provide total volume rates of change in the lagoon. The van der Meer and Janssen (VJ), European, and Hedges and Reis (HR) overtopping models were compared. The lagoon volume rate of change was compared to the predicted model rate of change for three different overtopping cases in 2006, 2008, and 2009. The models performed similarly with R^2 values of 0.72–0.86 for narrow banded cases, with an average reduction factor of 0.74.

THIS PAGE INTENTIONALLY LEFT BLANK

TABLE OF CONTENTS

THIS PAGE INTENTIONALLY LEFT BLANK

LIST OF FIGURES

THIS PAGE INTENTIONALLY LEFT BLANK

LIST OF TABLES

THIS PAGE INTENTIONALLY LEFT BLANK

ACKNOWLEDGMENTS

Thank you to Professor Edward Thornton and Professor Jamie MacMahan for spreading your enthusiasm of coastal oceanography. I learned so much from your experience and you made my experience at NPS very enjoyable. My office mates made life so much easier; Jenna Brown, Bill Swick and Mark Orzech, thank you for your help and guidance. Mike Cook, I appreciate the technical support and patience. I really appreciate the GIS support and surveying help from Arlene Guest and Jon Vevoda.

Finally, I would like to thank my husband, Michel. You have been so supportive, and helped me so much with my work. Thank you for your help with surveying and monitoring Carmel River Beach. I appreciate everything that you do for me.

THIS PAGE INTENTIONALLY LEFT BLANK

I. INTRODUCTION

A. BACKGROUND

Ephemeral rivers exist in locations around the world including South Africa, Australia, South America, India, Sri Lanka, Japan, Persian Gulf, U.S. West Coast, and Gulf of Mexico (Bruun, 1986; Largier et. al., 1992; Lanka Hydraulic Institute, 1997; Ranasinghe and Pattiaratchi, 2003; Stretch and Parkinson 2006; Baldock et al., 2008). Stretch and Parkinson (2006) summarized the climatology for the locations where ephemeral rivers tend to exist. These areas tend to have small tidal prisms, energetic waves, and low or intermittent river flow. They also usually occur in areas of steep, reflective beaches that act as barriers to an estuary.

Many species of plants and animals depend on the saltwater and freshwater estuary provided by the seasonal fluxes in ephemeral rivers. Kraus (2008) described the impact of these ecosystems in Northern California where they are habitats for many threatened or endangered species including steelhead trout, red-legged frogs, tidewater Goby, and Pacific salmon. The opening and closing of these estuaries is important for various species by both maintaining lagoon water elevation for maturation of juveniles and for the opening of the lagoon into the ocean for release and spawning.

The three phases of an ephemeral river system are: 1) filling of the lagoon by river inflow and/or wave overtopping, 2) breaching of the lagoon and river discharge through the formed inlet, and 3) closing of the river by waves during low flow. The water level and salinity concentration of the lagoon is dependent on the amount of river inflow and ocean wave overtopping. During coincident high waves and tides, overtopping of the barrier beach can cause water levels in the lagoon to rise. Overtopping and run-up play an important role in the building of the beach berm, which influences the potential for flooding the lagoon (Matias et al., 2009). As the lagoon level rises to a critical level, the lagoon may flood before it breaches naturally.

River inflow and wave overtopping from the ocean into the lagoon contribute to the seasonal breaching of the barrier beach. On the California coast, where the study site resides, breaching mostly occurs from the lagoon side during heavy precipitation events (Kraus, 2008) when river flow is strong enough to breach the beach. Most breaches occur rapidly by overtopping or by seepage through the barrier and reach maximum dimensions within several hours of opening. Surface water will erode a small channel between the lagoon and the ocean. Seepage through the berm is forced by differences in water elevations between the lagoon and the ocean (Kraus et al., 2002). These breaches can occur on a timescale on the order of hours by large storm waves and heavy precipitation. Ephemeral channel breaches tend to erode to a depth at mean sea level (Kraus, 2003). The outflow of a river can transport large amounts of sediment offshore affecting local turbidity of the nearshore zone and modifying the bathymetry. Kraus et al. (2002) found an ebb shoal was generated during a breach. Ephemeral rivers tend to remain open when streamflow is high, and tend to close when streamflow is low. Coastal breaching is expected to become more common with increasing sea level and erosion that tends to narrow the barrier beach (Kraus, 2003).

Many communities surrounding lagoons manually breach barrier beaches when the lagoon levels become too high in order to prevent flooding of properties. These manual breaches have both political and ecological impacts that need to be balanced. When the lagoon is breached, it can result in complete emptying of the lagoon, causing degradation of scenic views, areas for recreation, and habitats for the ecology. A beach can be manually breached by digging a small channel that will continue deepening and widening as the river scours a channel in the beach. (Kraus, 2008).

Breaching of barrier islands and temporary closed tidal inlets involve similar processes to beach breaching (Basco and Shin, 1999; Smith and Zarillo, 1988; Battilo et al., 2006). The breaching of earth-fill and impermeable dikes, which also act as a barrier to ocean processes, has been studied as well (Visser, 1998; Kraus, 2003; Reeve et al., 2008; Tuan et al., 2008).

Breach closures occur when river flow becomes too low to transport sediments from the river channel that are forced onshore by the ocean waves. The breach closure is forced by sediment overwash from wave run-up and overtopping (Kraus, 2008). Baldock et al. (2008) examined intermittently closed lagoons in South Wales, Australia from when they first breached to study the berm growth that takes place due to sediment overwash. They developed a morphodynamic model for berm growth on beaches combining previous wave run-up and sediment transport models. Basco and Shin (1999) developed a set of 1-D, numerical models for the three stages of barrier breaches including, storm surge, beach morphology, overwash and overland flow, storm tidal flooding from the ocean to bay, and storm tidal ebb from the bay to the ocean.

B. CARMEL RIVER/LAGOON SYSTEM

Carmel River State Beach, located on the Carmel Bay in Central California, acts as a barrier beach for the Carmel River that flows into the Carmel River Lagoon (Figure 1). This area is popular for recreation, scenery, and was designated as an Area of Special Biological Significance by the California Legislature in 1974. The Carmel River is part of a 660 km^2 watershed and is the largest tributary that flows into the Carmel Bay, providing freshwater inflow into the lagoon. The Carmel River is ephemeral that flows into the lagoon during the rainy season, generally January to June. During summer and fall when the river flows are low, waves build up the barrier beach that closes off the lagoon from the ocean. In the winter, when storms bring enough rain into the watershed, the river begins to flow raising the lagoon level. The flooding of the lagoon also occurs from the ocean side when storm waves, at high tide, overtop the barrier beach, which generally starts in October or November. When a critical flood stage in the lagoon is reached, there is enough force to breach through the barrier beach to form a channel that opens into the ocean (James, 2005).

Without manual breaching, the beach may not breach naturally in time to prevent flooding of the houses along the periphery of the lagoon. Since the early 1900s, the State and Monterey County have manually breached Carmel River State Beach to prevent flooding of the lagoon. The floodplain surrounding the lagoon is approximately 120

hectare; however, houses were built within this area before modern floodplain regulations. Breaching the lagoon can cause a 40–90 hectare-m drop in lagoon volume. After the initial breach, the lagoon will then continue to open and close either naturally or manually dependent of the river inflow (James, 2005).

Manual breaching can disrupt the natural levels of the lagoon that certain animal species depend on for survival. However, minimizing manual breaching is difficult due to the high risk of flooding to neighboring properties within the community. Recently, the river flows have been significantly reduced by withdrawals from Carmel River, which is the main water source for the Monterey Peninsula. Approximately 1850 hectare-m of water has been withdrawn each year from the river system, which reduces the ground water and surface inflow into the lagoon and causes it to be dry most summers (James, 2005).

With this drying of the Carmel River, environmental agencies have been concerned with the habitat of several threatened species in this area, including the red-legged frogs, steelhead trout, and other threatened species that are protected by the Endangered Species Act (James, 2005). The National Oceanic and Atmospheric Administration (NOAA), National Marine Fisheries Service (NMFS), and the California Department of Fish and Game (CDFG) propose to manage manual breaching of the lagoon to maintain adequate water levels in order to protect fish and wildlife habitat in the lagoon (James, 2005).

The timing and location of the breach is important for maintaining water levels in the lagoon. Carmel River beach is constrained on both sides by granodiorite outcrops with beach in between (Figure 2). The beach width depends on the season, but the northern end is normally wider than the southern end (Storlazzi and Field, 2000). The lagoon level fluctuations are dependent on the location of the outflow channel. The river outflow is constrained when flowing at the north or south ends of the beach by rocky outcrops providing a bottom sill acting as a weir. In between, the depth of sand goes down to 180m, and the depth of the river channel is unconstrained, so that if the breach occurs here, the lagoon tends to empty. There have been trials to determine the best outflow channel location to maintain adequate lagoon levels. The breaches that occur

farther to the north maintain higher freshwater lagoon levels because of a higher sill, but can result in increased dune erosion along Scenic Road as occurred in 1993, 1997, and 2005 (James, 2005).

Field data and observations for Water Years (WY) 1991–2005 were analyzed by James (2005) to determine the hydrologic and oceanic influences, including how the lagoon responds to river inflows, outflows and ocean forces. He found that the river inflow of 6 m^3/s was adequate maintaining the breach in the beach. With an inflow rate less than 3 m^3/s, there will be intermittent closures and openings. When the inflow rate reaches below 0.3 m^3/s, the river mouth will remain closed. Once the river is closed for the dry season, a dynamic equilibrium exists between the lagoon inflow, evapotranspiration and seepage. Lagoon equilibrium occurs when a surface inflow rate of 0.2 m^3/s is offset by lagoon seepage and evapotranspiration. The lagoon level usually reaches its lower limit of 1.6m (NAVD88) during late summer, around August (James, 2005). All of the vertical heights are relative to the NAVD88 datum.

The focus of this paper is to describe measurements and modeling flooding of the lagoon by wave overtopping as a first step in the development of a comprehensive model of ephemeral rivers. Little comprehensive field data are available for ephemeral river processes. In Chapter II, unique data on lagoon elevation, river inflow, and wave processes are presented. In Chapter III, previous models of wave run-up and wave overtopping are described followed by the results of the application of the models and comparison with data in Chapter IV. Discussion and conclusions are presented in Chapters V and VI.

THIS PAGE INTENTIONALLY LEFT BLANK

II. DATA

A. WAVES AND TIDES

The wave data were obtained using the Coastal Data Information Program (CDIP) wave spectra. Deepwater directional wave spectra are measured offshore by buoy #157 located off of Point Sur at 36 20.27N 122 06.08W (Figure 1). The buoy is a Datawell Mark 3 buoy with an accuracy of 0.5% full scale and ~0.5deg in directional error. The measured spectra are refracted to obtain nearshore spectra at CDIP Monitoring Prediction System (MOP) location MO634 located in 15m water depth directly offshore of the river mouth at 36 32.10 N 121 56.05 W (Figure 1). Additional error is associated with the CDIP linear spectral wave propagation model. The nearshore directional spectra at the 15m depth are collapsed into one-directional energy spectra $E_{15}(f)$ and are back-shoaled to obtain offshore 1-D wave spectra, assuming conservation of energy,

$$E_0(f) = \frac{c_{g15}(f)}{c_{g0}(f)} E_{15}(f) \qquad (1)$$

where subscript (0) refers to deep water and $c_g(f)$ are the respective group velocities calculated using linear wave theory. It is interesting to note that in 15m water depth the group velocity slows across the energetic part of the wave spectrum from 0.04 to 0.25Hz, which results in offshore wave heights being greater than those at the 15m depth owing to shoaling effects only.

Assuming the waves are Rayleigh distributed, the significant wave height offshore, $H_S = 4\sigma$, where σ^2 is the surface elevation variance obtained as the area under the back-shoaled offshore wave spectrum. The average wave period, T_{m0}, is calculated from the zeroth moment divided by the first moment of the energy spectrum. Deepwater wavelength is calculated using linear wave theory, $L_0 = gT^2 / 2\pi$.

The tides are obtained from NOAA for Monterey, CA station 9413450. According to NOAA and the National Ocean Survey (NOS), Carmel River Beach tides lag Monterey by less than 5min, which is assumed negligible. The accuracy of the NOAA tides is +/- 0.02m. The tides are in GMT time and have a vertical datum of NAVD88 in meters.

B. LAGOON VOLUME

Carmel River inflow into the lagoon is calculated from river stage measurements obtained using a pressure transducer/data recording system at the Highway 1 Bridge (Figure 2). The Monterey Water Management District computes mean daily streamflow values from these stage data with a stage discharge relation table using USGS techniques (James, 2005).

The lagoon heights are measured on the south branch of the lagoon every 15 minutes with a pressure gage compensated for by measured barometric pressure (Figure 2). The accuracy of the lagoon elevation measurements is 0.015 m by comparison to a staff gage (James, 2009). The heights are measured in NGVD29, but were converted to NAVD88 in meters with a conversion of +0.833m, a conversion based on lat/long according to the National Geodetic Survey (NGS) orthometric height conversion tool (NGS, 2009).

The lagoon volumes, V, are calculated using a stage-volume curve (Hope, 2007), with the measured lagoon heights. The stage volume curve was developed from 4 different lagoon surveys with the least vertical accuracy of +/-0.3 m. The least accurate for the main stem of the lagoon was +/-0.15 m. A third-order polynomial was fit to the stage-volume curve data and applied here in m^3,

$$V = 14491.48h^3 - 33323.69h^2 + 35041.08h - 7001.09 \qquad (2)$$

where h the lagoon water level.

The rates of volume change are obtained by center differencing the volumes at 15 minute intervals. A one-hour averaged rate of change is obtained using a 5-point running average.

C. BEACH MORPHOLOGY

Berm heights and beach slopes as determined from the beach morphology are input parameters to the run-up and overtopping models. Walking beach surveys were conducted (Table 1) using an Ashtech z-Xtreme GPS system, which has a horizontal accuracy of 1cm and vertical accuracy of 2cm. The surveys comprised of lines spaced ~20m. A criterion for considering an overtopping event is that the beach surveys preceded overtopping events by less than two weeks, 25Jan2009 (Case1), 16Oct2008 (Case 2), and 12Sep2006 (Case3). The National Geodetic Survey (NGS) GEOID99 model was used to convert the vertical heights to NAVD88 vertical datum.

Using linear interpolation of the survey data, berm height and beach slope were calculated from shore-normal beach profiles spaced every 5m alongshore (Figure 2). The beach slope was calculated by taking the average of one-meter increments of the profile for the steepest section of the beach closest to the shoreline. The berm height was calculated as the maximum elevation on the profile within 100m of the shoreline. Two sections of the beach were used that were each rotated in order for the y-axis to be parallel to the shoreline (indicated as box A and B in Figure 2).

THIS PAGE INTENTIONALLY LEFT BLANK

III. RUN-UP AND OVERTOPPING MODELS

A. RUN-UP

Run-up is the vertical distance above the still water level that a wave travels up a beach face. Overtopping occurs when run-up exceeds the berm height. Coastal engineers by convention have parameterized wave run-up in terms of the exceedence of the highest 2% of the wave run-up, $R_{2\%}$ (Pullen et al., 2007). A large number of both small and large scale laboratory studies have been conducted to measure run-up values for sloped dikes and seawalls (Hunt, 1959; van der Meer and Jenssen, 1995; Hedges and Reis, 1998; and others). Hunt (1959) empirically characterized run-up on a smooth slope as a function of offshore wave height, H , and Iribarren number, ξ ,

$$R = KH\xi \,, \tag{3}$$

where K is a constant and ξ is the Iribarren number defined as:

$$\xi = \frac{\beta}{\sqrt{H / L_0}} \quad . \tag{4}$$

The Iribarren number describes the waves breaking form as a function of beach slope, β , and wave steepness (Battjes, 1974). Hunt's relationship is the basis for subsequent run-up formulas. The following subscripts for the Iribarren number, ξ_{m0} and ξ_p refer to use of the average period or peak period used in the calculation for L_0 .

The European run-up model (Pullen et al., 2007) uses separate run-up formulas for breaking, ξ <2, and non-breaking waves, ξ >2;

$$\frac{R_{2\%}}{H_S} = 1.75\gamma_f\gamma_b\gamma_\theta\xi_{m0} \qquad \xi_{m0} \le 2$$

$$\frac{R_{2\%}}{H_S} = \gamma_f\gamma_\theta\left(4.3 - 1.6/\sqrt{\xi_{m0}}\right) \qquad \xi_{m0} > 2 \quad . \tag{3}$$

with reduction factors to account for non-normal wave incident angle (γ_θ), berm characteristics (γ_b), and surface roughness (γ_f) influence. The maximum run-up value occurs when all of these factors are equal to 1. The equations for these run-up formulas are parameterized on significant wave height at the toe of the structure as measured in the laboratory experiments; however, H_S offshore significant wave height would be used in the applications. The coefficients of the European formulas are based on a large international dataset from small and large scale laboratory experiments.

Fewer studies have concentrated on run-up on natural beaches (Holland and Holman, 1993; Raubenheimer et al., 1995; Ruggiero et al., 2004; Stockdon et al., 2006). Stockdon et al. (2006) utilized previous field study observations and represents run-up,

$$R_{2\%} = \overline{\eta} + \frac{S}{2} \quad , \tag{4}$$

as a function of both setup and swash, where $\overline{\eta}$ is setup, and swash, $S = \sqrt{{S_{inc}}^2 + {S_{IG}}^2}$, which has contributions from both incident, *inc*, and infragravity, *IG*, waves. Using data from 10 field experiments with varying bathymetries and wave heights, they empirically found

$$R_{2\%} = 1.1(0.35\beta(H_S L_0)^{1/2} + \frac{[H_S L_0(0.563\beta^2 + 0.004)]^{1/2}}{2} \quad , \tag{5}$$

where β is the foreshore beach slope. The deepwater significant wave height, H_S, is obtained by reverse shoaling from the measured wave heights in shallower water outside the surf zone for the various experiments. For reflective beaches (ξ >1.25), run-up is dominated by incident wave energy where the infragravity portion of run-up calculations is negligible (Guza and Thornton, 1982), and (5) reduces to the Hunt (1959) formula (1)

$$R_{2\%} = 0.73 H_S \xi_{m0} \quad . \tag{6}$$

The data set used to develop the model was limited to H_S <2.5m. They found that the model underestimated run-up heights by ~17cm.

B. OVERTOPPING

The overtopping empirical models are based on laboratory studies of overtopping of structures and not on natural beaches. The models are for design specification to limit overtopping of levees and dikes, and therefore give conservative values (Owen, 1980; Van der meer and Janssen, 1995; Pullen et al., 2007; Goda, 2009). Crest height refers to the top of a man-made structure, where berm height refers to the top of a beach berm, although both have the same function. A beach can act in the same manner as these structures, protecting the back bay from wave attack and flooding. The models are 1D models applied in a quasi-2D approach by dividing the beach into 35 different sections every 5m across the beach, each having different beach slopes and berm heights.

Wave overtopping values depend on the ratio between freeboard height and wave run-up height. Freeboard, R_c, is defined as the height of the berm crest above the mean water level. In order for waves to overtop a berm, the run-up heights must be greater than the freeboard height. Overtopping is dependent on the run-up height, and therefore dependent on incident wave height, period, and beach slope.

A number of empirical models have been developed utilizing laboratory data and dimensional analysis. The various proposed empirical models use different non-dimensionalizing parameters. As pointed out by Hedges and Reis (1998) dimensional analysis suggests certain parameterizations, but they are not necessarily unique, correct, or physically based. Owen (1980) proposed an exponential relationship for overtopping discharge, Q, as a function of freeboard height, R_C, wave height, and mean wave period for simple structures with uniform slope,

$$\frac{Q}{T_{m0} g H_S} = A \exp\left(-B \frac{R_C}{\gamma_r T_{m0} \sqrt{g H_S}} \right) \tag{8}$$

where g is gravitational acceleration and include the same reduction factors as in the run-up formulas and add the influence of a shallow foreshore with the effect of all reduction factors annotated as γ_r. The coefficients A and B were determined from five laboratory experiments with uniform slopes of 1:1, 1:2 and 1:4 consisting of 100 waves each.

Besley (1999) revised the coefficients for Owen's model. A deficiency of the exponential form is that nonzero discharge is predicted for all finite freeboard heights. Only when the freeboard height is infinite does the overtopping rate go to zero.

Van der Meer and Janssen (1995), referred to as the VJ model, proposed exponential overtopping formulas using a different non-dimensional form for breaking and non-breaking waves.

$$\frac{Q}{\sqrt{g H_S^{\,3}}} = \frac{A}{\sqrt{\beta}} \xi_p \exp\left(-B \frac{R_C}{\gamma_r \xi_p H_S} \right) \qquad \xi_p \le 2 \qquad (9)$$

$$\frac{Q}{\sqrt{g H_S^{\,3}}} = C \exp\left(-D \frac{R_C}{\gamma_r H_S} \right) \qquad \xi_p > 2$$

where the significant wave height at the toe of the structure, H_S and T_p are used. Again the coefficients are empirically specified using laboratory data where A=0.06, B=5.2, C=0.2, D=2.6. The European overtopping model of the same form (Pullen et al., 2007) uses an expanded dataset incorporating various experiments to modify the coefficients in (Equation 9) with A=0.67, B=4.75, C=0.2, and D=2.6. The European model uses T_{m0} in place of T_p.

Hedges and Reis (1998), referred to as HR hereafter, developed a semi-empirical model with the form of the model based on the physical equation for discharge over a weir as analogous to discharge over a berm. They impose the conditions that 1) wave overtopping equals zero when the freeboard is greater than the crest elevation, and 2) when there is no freeboard, the overtopping discharge remains finite, and obtain:

$$\frac{Q}{\sqrt{g R_{\max}^3}} = \begin{cases} A\left(1 - \dfrac{R_C}{\gamma_r R_{\max}}\right)^B & for\ 0 \le \dfrac{R_c}{\gamma_r R_{\max}} < 1 \\ 0 & for\ \ \dfrac{R_c}{\gamma_r R_{\max}} \ge 1 \end{cases} . \qquad (10)$$

They use Owen (1980) overtopping data to determine a maximum run-up value, $R_{\max}$, for which no overtopping occurs, which is the objective of the design formulas. They point

out that under random wave conditions, overtopping will be dominated by a few waves with large run-up and that if R_C is substantial, most waves will contribute no overtopping. From the data, assuming a Rayleigh distribution for run-up and using the formulas by Allsop et al. (1985) to calculate run-up, they found that the most probable maximum run-up that did not exceed R_C corresponded to a value not exceeded in 37% of the cases for a Rayleigh distribution of run-up for 100 waves, referred to as $R_{max37\%}$. They then proceed to obtain the coefficients of the overtopping model from the experiments. The model is parameterized with, T_p, and, H_S.

Mase et al. (2003) extended the HR model (Equation 10) to include a modified version of Hunt's run-up equation that included wave set-up that they calibrate with additional Japanese data that includes shallower slopes up to 1:20. Reis et al. (2008) restated the modified run-up using $R_{\max 37\%}$,

$$R_{\max 37\%} / H_S \approx \begin{cases} 0.38 + 1.67\xi_p & for 0 < \xi_p \le 2.2 \\ 4.56 - 0.23\xi_p & for 2.2 < \xi_p \le 9.0 \\ 2.51 & for 9.0 < \xi_p \end{cases} . \qquad (11)$$

Additionally, the coefficients of the HR model (Equation 10) were modified by Reis et al. (2008) using the expanded combined Owen (1985) and Japanese data set,

$$A = \begin{cases} 0.0033 + 0.0025(1/\beta) & for 0.08 \le \beta \le 1 \\ 0.0333 & for 0.05 \le \beta < 0.083 \end{cases}$$
$$B = \begin{cases} 2.8 + 0.65(1/\beta) & for 0.13 \le \beta \le 1 \\ 10.2 - 0.275(1/\beta) & for 0.05 \le \beta < 0.13 \end{cases} . \qquad (12)$$

These modifications are added to the HR model and will be referred to as such.

THIS PAGE INTENTIONALLY LEFT BLANK

IV. RESULTS

The rates of wave overtopping into the lagoon are equated to the volume changes of the lagoon when there was no river inflow. The overtopping rate data are compared with the European (Eq. 9), VJ (Eq. 9), and the modified HR (Eq. 10–12) overtopping models. Parameter ranges for ocean, lagoon, and beach morphology data during the times of overtopping for Cases 1–3 are shown in Table 1. The coefficient of determination, R^2, and linear regression slope are used to describe the correlation between the models and data for each case. In order for the linear regression slope ~1, the reduction factors, γ_r in the models are adjusted. These new values for R^2 are shown in Table 2. The lagoon height error, +/- 0.015m, were added and subtracted from the initial lagoon height values and then the same methods were used to determine volume rate of change. These are displayed as error bars on the overtopping plots. The errors increase with increasing overtopping rates because the two values increase in separation with a higher rate of change.

A. CASE 1

The 07 February 2009 overtopping event used the 25 January 2009 beach survey for morphology information. The lagoon height increased 0.16m that resulted in an increase of 2.47 x10^4 m^3 in volume over an 11 hour period. The greatest overtopping rate of 2.39 m^3/s occurred at 1600, which coincided with the peak tide height. The maximum wave height was the highest of all three cases at 3.1m. The wave spectra before the overtopping event is broad-banded, becoming narrower banded as the overtopping increases with a smaller peak at a lower frequency.

All models over predict the overtopping in this case with regression slopes of 2.8–6.18 (Table 2). The models were then adjusted with a reduction factor so that the regression slope ~1. The reduction factors ranged from 0.66–0.79 for the three models.

The R^2 values for the tuned models ranged from 0.83–0.86 (Table 2). The models more accurately predict the overtopping rates after the peak overtopping rate at 1600 (Figure 4).

B. CASE 2

The 26 October 2008 overtopping event used the 16 October 2008 beach survey for morphology information. The lagoon height change was approximately 0.082m in 9 hours, which is equivalent to 7.49×10^3 m^3 of volume change. The height increase was approximately two times smaller than Case 1, resulting in a volume increase that is ~3.3 times smaller. The wave spectra are narrow banded with a peak period around 18sec (Fig 3) with maximum offshore significant wave heights ~1.7m, resulting in low slope waves and ξ=1.04–2.84.

Both the European and the HR model estimation peaks are at the same time as the maximum tidal heights. The maximum overtopping rate was 0.66 m^3/s. All of the models over-predict the overtopping rate throughout the event with regression slopes of 3.48 to 4.41. After the reduction factors are applied, the models over-predict the overtopping during the first four hours of the event that coincides with when T_p and T_{m0} are greater (Figure 5). Better correlation with the data occurs after the maximum overtopping rate at 0500. The reduction factors ranged from 0.73–0.81 for the three models. The R^2 values ranged from 0.72–0.86 with the European model performing the best with R^2=0.86.

C. CASE 3

The wave spectra for the 20 September 2006 overtopping case are broad-banded with a maximum wave height of 1.8m. The average wave height and periods are less than in the other two cases (Figure 3). The models in this case under predict the overtopping rates with regression slopes of 0.09–0.56 (Figure 7). Reduction factors could not be applied because the models predicted less than the overtopping rate (Figure 6, upper panel).

When the peak period used in the overtopping models was shifted to the lower peak in the spectra (Figure 3) at 12.5s, the model correlations improved significantly (Figure 6, middle panel; Table 2). The correlation for the European model did not improve because only T_p was adjusted. If the periods used were increased and had narrowband wave spectra at lower frequencies like the other cases, then the models would predict more overtopping.

D. MODEL SENSITIVITY

The sensitivity of the European and the HR models to the input parameters are shown in Figure 8. The VJ model has the same functional form as the European model and differs only by parameterization using T_p instead of T_{m0} and different coefficients. Therefore, the VJ response to model parameters is similar to the European model and not shown. According to Goda (2008), the most important parameter in the overtopping models is the freeboard height. This is because if the freeboard is greater than the maximum run-up height then overtopping is not physically possible.

These models are also dependent on wave height, wave period, and beach slope (Eqs. 9–12). In the sensitivity plots, each parameter was plotted individually versus the European and the HR model. While one parameter varied, the other the parameters were held constant at T = 12s, R_C = 2, H_S = 2, β = 0.1, and γ_r =1. The models increase exponentially with increasing wave height, wavelength, and beach slope. With respect to freeboard, overtopping decreases exponentially.

The run-up sensitivity is also shown in the lower panel of Figure 8. The run-up increases approximately linearly with wave height, period, and beach slope. It is interesting to note that the HR run-up values are higher than that of the European; however, the HR overtopping values are less than that of the European. The Stockdon model predicts less run-up than both the European and HR models.

THIS PAGE INTENTIONALLY LEFT BLANK

V. DISCUSSION

Data uncertainty exists from measuring the lagoon height to calculate the volume based on a stage volume curve. The stage volume curve used to convert lagoon height into volume is based on survey data from 2003–2007 and likely to have changed owing to bathymetry changes in the lagoon. Error is associated with measuring the lagoon height and with the stage-volume curve. The non-linear shape of the stage-volume curve causes a larger error with greater lagoon volumes.

Other factors of the lagoon water balance equation were not included in this model. The groundwater inflow rate into the lagoon is unknown but is likely to occur due to higher water levels in neighboring groundwater monitoring than in the lagoon. Subsurface inflows (or outflows) also occur through the sand bar, which could be driven by differences between lagoon level and mean sea level changes by wave set-up and tides (Watson, 2004). Precipitation and evaporation into the lagoon were assumed negligible during the approximate 6 hour overtopping episodes.

A time lag occurred between the lagoon volume change and the maximum tide height. The lagoon volumes were shifted back by one hour in each case to account for this unknown time lag. This could be due to data error or due to a physical lag such as initial decreased run-up until the berm is fully saturated by water. Tides measurements were used from the tidal station at Monterey and the Carmel River Beach tides may lag more than expected.

Model errors occur owing to errors of input parameters including wave height, wave period, tide elevation, and beach morphology. Wave height errors of approximately 10% are associated with measurements by the wave buoy and with refraction of the waves from offshore to the 15m depth using the CDIP refraction model. The models use different input wave heights. The HR model is parameterized using offshore wave height, as presented here. However, the European and VJ models are parameterized to use wave height at the toe of the structure, which is difficult to calculate or measure. Instead, the offshore wave height was used in the European and VJ model applications

here. The offshore wave height accounts for nearshore refraction on bathymetry. The wave period error is associated with the spectral resolution, and ranges 0.5–2.0 seconds over the peak period range of 10–20 seconds.

The models were parameterized with different run-up distribution values. The European and VJ models uses $R_{2\%}$, whereas the HR uses $R_{\max 37\%}$. Reis et al. (2008) points out that if the Rayleigh distribution applies to run-up, $R_{\max 37\%}$ is equivalent to $R_{1\%}$ and that the earlier utilized $R_{2\%} = 0.93\ R_{1\%}$. This is a reason the HR run-up values are greater than those of the European model.

The models were derived for smooth impermeable plane beaches in the laboratory. Carmel River Beach mean grain size is 0.62mm composed mostly of quartz (Storlazzi and Field, 2000) and is a permeable, uneven surface. The models are also calibrated with plane straight slopes, where beach slopes vary and have curvature. For these reasons the models predicted run-up values and subsequent overtopping rates are expected to be too large. The over-prediction is accounted for by applying reduction factors.

The beach segment of Carmel River Beach used to calculate overtopping was 175m in length bounded by the parking lot to the north and a headland to the south (Figure 2). This location was assumed the most likely for overtopping to occur. Overtopping events are corroborated by photographs. The beach morphology used in the models was measured 10–13 days prior to the overtopping events. The morphology may have changed during this time period to affect the results of the model.

The Stockdon et al. (2006) model, based on field measurements, appears to significantly underestimate run-up, as it predicted almost no run-up greater than the berm height, i.e. no overtopping. The Stockdon et al. (2006) model for reflective cases, ξ>1.25, reduces to Hunt's equation (Eq. 6). The multiplier is 58% smaller than for the European and HR model resulting in reduced predicted run-up. A possible reason is that the Stockdon model consisted of 91% Duck data. Because it is a barred beach, much of the wave energy is dissipated on the bar and not on the beach. They use offshore significant wave height back refracted from measurements in 8m, which do not account

for dissipation on the bar. Therefore, the wave heights used in their empirical model are too large compared with the run-up at the beach, i.e. the run-up is predicted too low for the given offshore wave height. The data used in the model corresponding most closely to Carmel River Beach is from San Onofre, California, which is a reflective beach with long period incident Pacific swell; however, this data set did not have large wave heights.

The lab data consists of profiles composed of a shallow or horizontal sloping bed joined to a steep beach. Carmel Beach profiles have a shallow sloping offshore profile and a steep beach face slope similar to the laboratory cases. Therefore, it would be expected that the Carmel beach run-up might be better simulated using the laboratory data based model rather than the Stockdon et al. (2006) model.

A reason the laboratory derived empirical run-up and overtopping formulas may have worked well is that the laboratory data and Carmel River Beach are relatively steep beaches. The Iribarren number for the data acquired at Carmel River Beach ranged $1 < \xi_p < 3$, indicating the beach is reflective. The laboratory data for which the overtopping formulas were developed had beach slopes ranging $0.05 \le \beta \le 1$ indicating the beaches were reflective.

Goda (2009) finds that non-normal incident waves to the beach can significantly reduce the run-up. The reason is that the slope of the beach is effectively reduced when the wave runs up the beach at an angle and run-up decreases with decreasing slope. The waves that are incident to Carmel River Beach must come through a limited aperture bounded by the Point Lobos Headland to the south and the rocky reef just to the north of the beach. This limits the wave incidence offshore such that the waves arriving at the beach ~ <5 degrees after nearshore refraction. For the three cases, the measured angle of incidence at the 15m depth was $\le 15^\circ$ (Table 1). Assuming refraction over straight and parallel motions, the incident angle in 2m (approximate depth) would be $\le 5^\circ$. For small angles, the EurOtop Manual recommends

$$\gamma_r = \begin{cases} 1 - 0.0033|\theta| & 0^\circ \le |\theta| \le 80^\circ \\ 0.736 & |\theta| > 80^\circ \end{cases} , \qquad (13)$$

where θ is the angle of wave attack. Goda finds for waves with different angles of attack, that the reduction factor has the following regression curve,

$$\gamma_r = 1 - 0.0096|\theta| + 0.000054\theta^2 \quad , \quad (14)$$

which indicates a decrease in the reduction factor with the angle of wave attack. For a 5° wave angle the reduction factors would be 0.98 and 0.95 for Equations 13 and 14 respectively.

In Case 3, the wave energy was broad-banded and with less energy than the other cases. The spectra included one large and one small peak periods. This case showed the worst model performance of the three cases with under-prediction of overtopping rates. When the period at the lower frequency peak, 12.5, was input into the models, the performance increased significantly. This shows that the long period wavelengths are important in overtopping and may cause the most amounts. The mean period does not affectively provide an accurate depiction of the longer period waves that may be occurring. Therefore, narrow-banded wave energy spectra for these models more accurately predict overtopping.

The European overtopping model was derived from the VJ model so they behave similarly only with different coefficients. They were compared to show the difference of overtopping predictions when using T_{m0} and T_p. The VJ model that uses T_p did not do as well as the European model for Cases 1 and 2. However, the European model digresses when using the low frequency energy peak in Case 3. The HR and European model both performed similarly despite the fact that they use different periods. The models predict more overtopping in Case 1, but also more overtopping occurs throughout the event (Figure 7). In Case 3, the regression slopes indicate under prediction of the overtopping rates. The reduction factors for the European and HR model for both Case 1 and Case 2 are close to 0.77. This reduction factor for both models is due little to wave direction, but mostly for slope variability, berm permeability and roughness. The reduction factors were calibrated for Carmel River State Beach, a natural, reflective beach with a specific sand size.

A. FUTURE WORK

Future plans for the Carmel River Beach are to improve the overtopping flood model with additional data. Continual beach surveying will be done to continue to monitor morphology changes and breaching events. The most efficient way to monitor beach changes, overtopping, and breaching events would be to install a video camera for constant monitoring. A new stage volume curve with new bathymetric surveys could improve model accuracy. As the groundwater is an unknown factor in the lagoon volume water balance, this would be helpful to measure and monitor. With continued research on ephemeral rivers, a breaching model could be developed. A planned next step is to implement the 2-dimensional morphodynamic model X-Beach to study the full breaching process.

THIS PAGE INTENTIONALLY LEFT BLANK

VI. CONCLUSIONS

Ephemeral rivers are important areas around the world for flooding and breaching of barrier beaches. A wave overtopping model was investigated for predicting barrier breaching and flooding at the Carmel River State Beach in Carmel, CA, an ephemeral river that seasonally breaches. Lagoon elevation changes of the Carmel Lagoon were used to calculate overtopping rates for three case studies with recent beach survey data.

The European, VJ and HR overtopping models were used to predict these overtopping rates based on offshore wave heights, hourly tides, peak period, mean period, beach slope and berm height every 5m across the length of the beach. The Stockdon et al. (2006) run-up model for natural beaches was inputted into the HR model, however, these values were too small to indicate significant amounts of overtopping. It is concluded that the Stockdon et al. (2006) model significantly underestimates run-up, at least for the cases considered here. Instead, the Reis run-up model was used to modify the HR model. Both the European model using mean period and peak period with the VJ coefficients were compared. The models correlated with the overtopping data although over predicted the overtopping rates by 3.0–6.7 times, with the VJ model over-predicting the greatest.

Reduction factors were used to fit the model to the data by obtaining a regression slope of~1. For Case 1 and 2, the reduction factors ranged between 0.66–0.81, with the VJ model being adjusted the most. The R^2 values ranged from 0.72–0.86, and the European model performing the best with R^2 values of 0.86. In Case 3, the wave spectra were more broad-banded, therefore the models did not perform well until a longer peak period of 12.5sec was selected. The HR and VJ models that both use T_p performed significantly better with R^2 values of 0.87 and 0.84. This shows the importance of long period waves in overtopping. Overall, the three models performed similarly, but is recommend to use peak period inputs for cases like in Case 3.

THIS PAGE INTENTIONALLY LEFT BLANK

APPENDIX A. FIGURES/TABLES

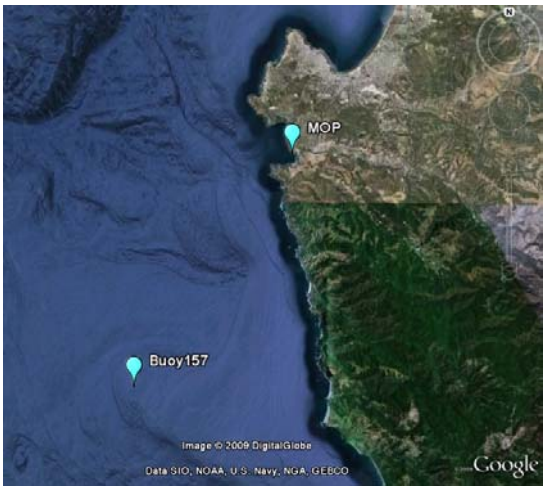

Figure 1. Area map off the coast of Carmel, California. CDIP Buoy #157 provides the wave height and period measurements for the model that refracts wave to the MOP station (from Google Maps last accessed 27 August 2009).

Figure 2. Area map of Carmel River State beach. Broad area map on left indicates location of the lagoon height measurements and the river inflow measurements. Blow up of beach with two boxes used to calculate slope and berm heights for overtopping models (from Google Maps last accessed 27 August 2009).

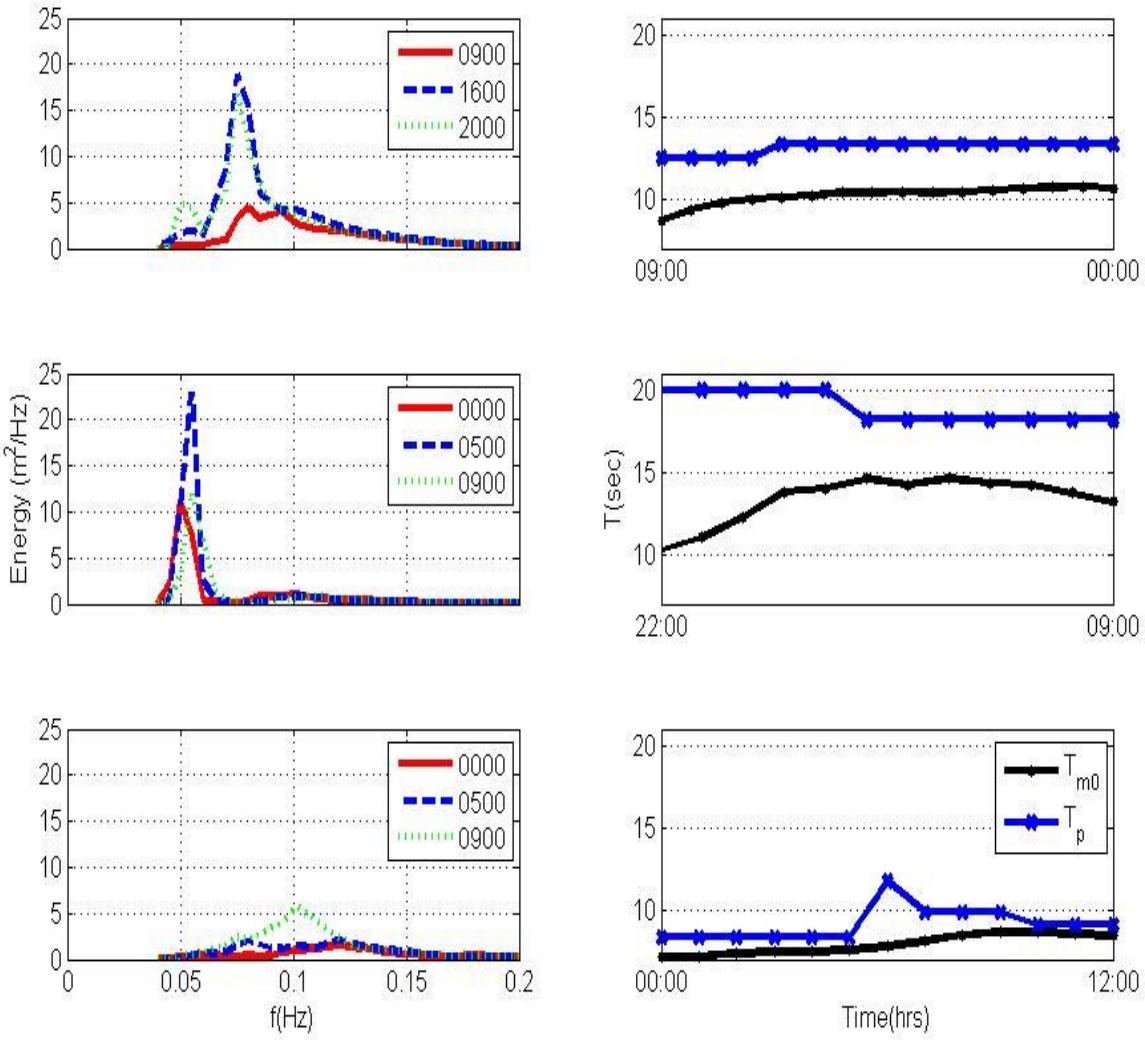

Figure 3. Wave spectra are the left column and wave T_p and T_{m0} are in the right column. Case 1, 2, and 3 are in rows 1, 2, and 3 respectively. Wave spectra are shown evolving in time during the overtopping event. There is much less wave energy in Case 3 along with shorter wave periods. T_p is around 19s for Case 1 and around 13s for Case 2.

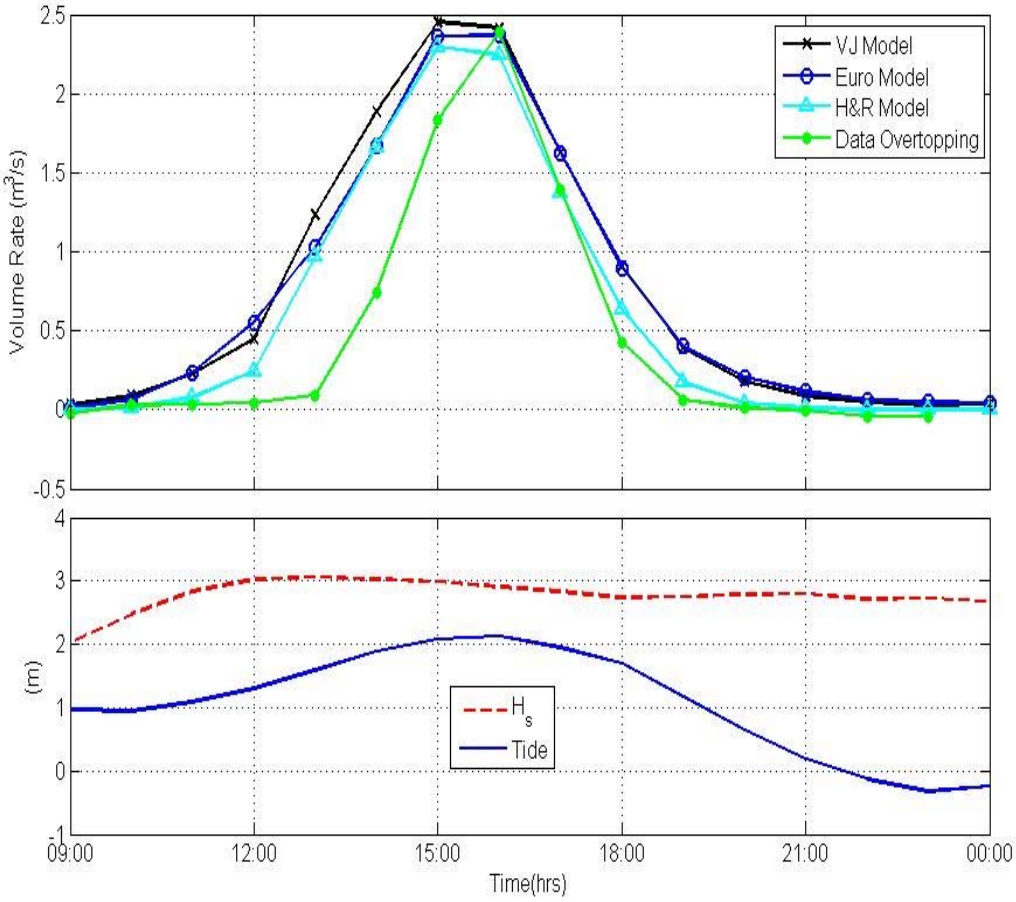

Figure 4. Overtopping Case 1 event 07 February 2009. Comparison of the overtopping models with the calculated overtopping rates. The models were plotted after including the reduction factors listed in Table 2. Wave height and tides for the same time period are below.

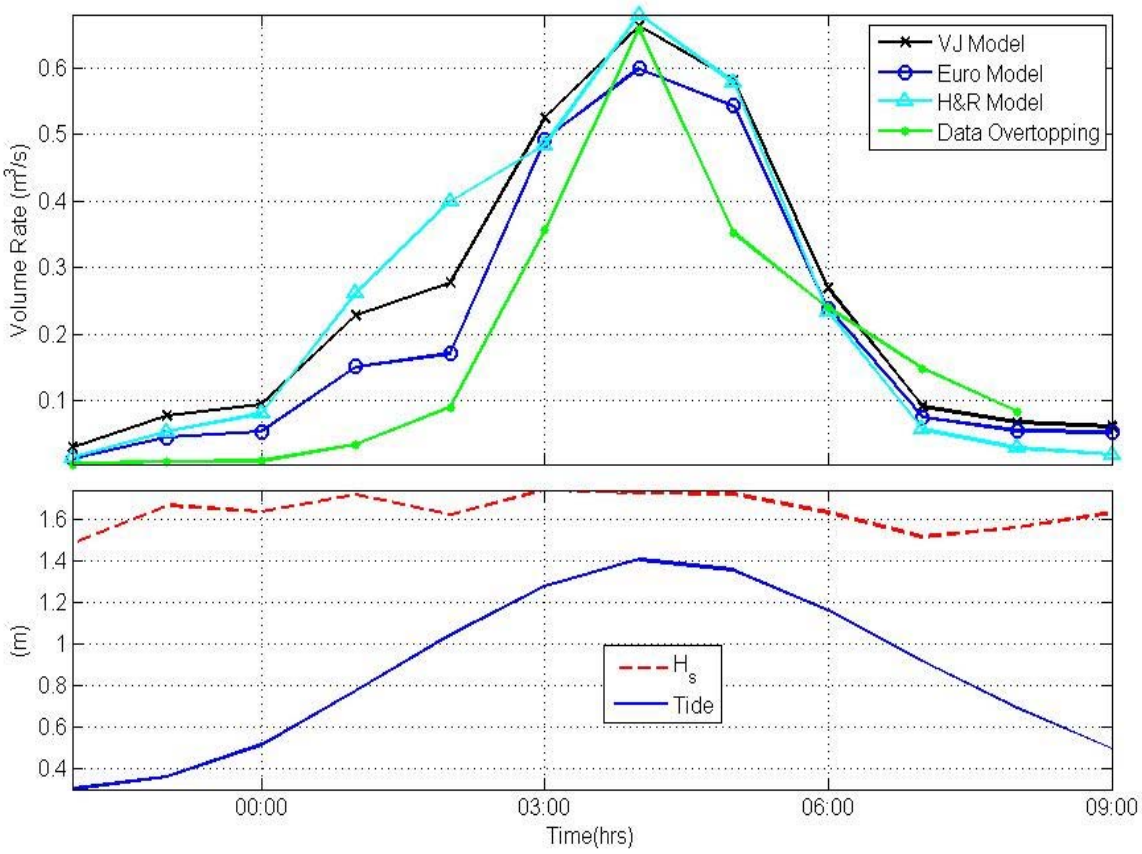

Figure 5. Overtopping Case 2 event 26 October 2008. Same as Figure 4, note different scales.

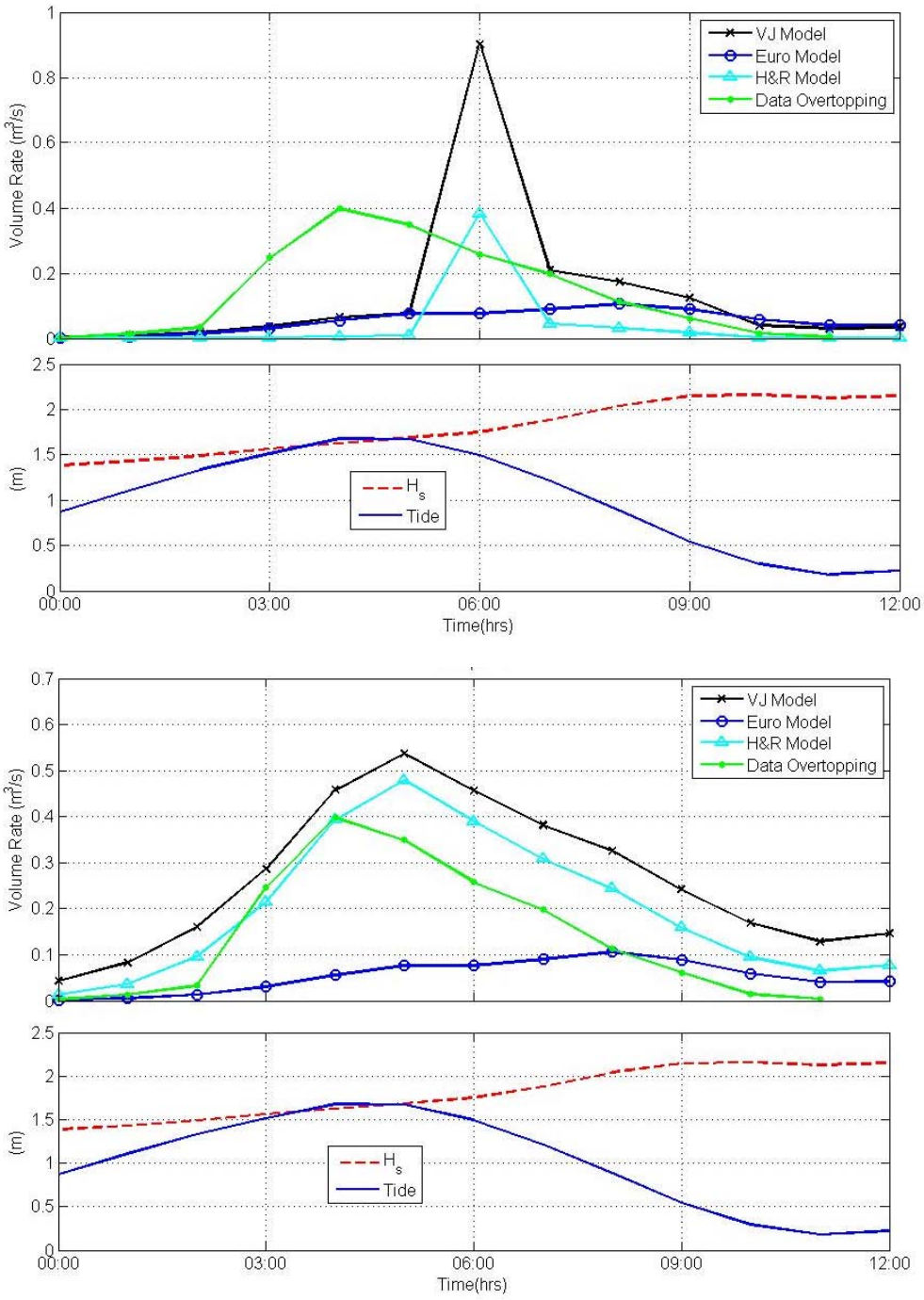

Figure 6. Overtopping Case 3 event 20 September 2006. Same as Figure 4, note different scales. The bottom figure is the same plot when T_p =12.5 was used.

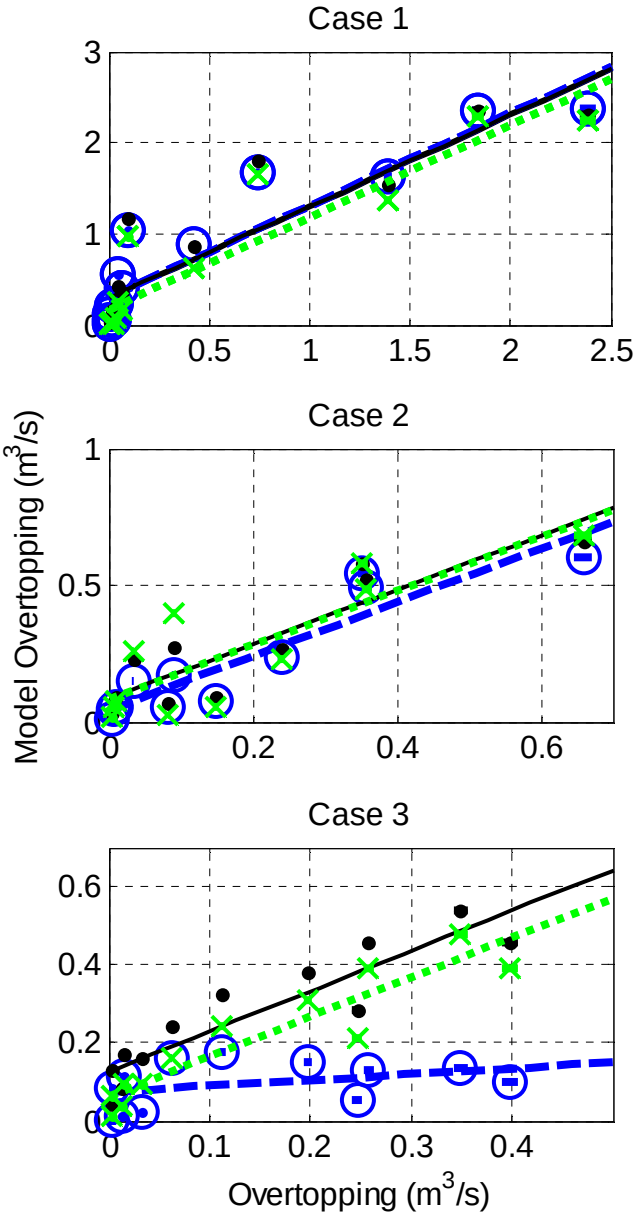

Figure 7. Case 1, 2, and 3 overtopping rates versus the European (dashed lines, open circles), VJ (lines, dots), and HR (dotted line, x's) overtopping rates. The error bars to account for the lagoon measurement errors are included in the data overtopping rates. These increase with increasing overtopping rate. The regression lines for each model are plotted to show slopes.

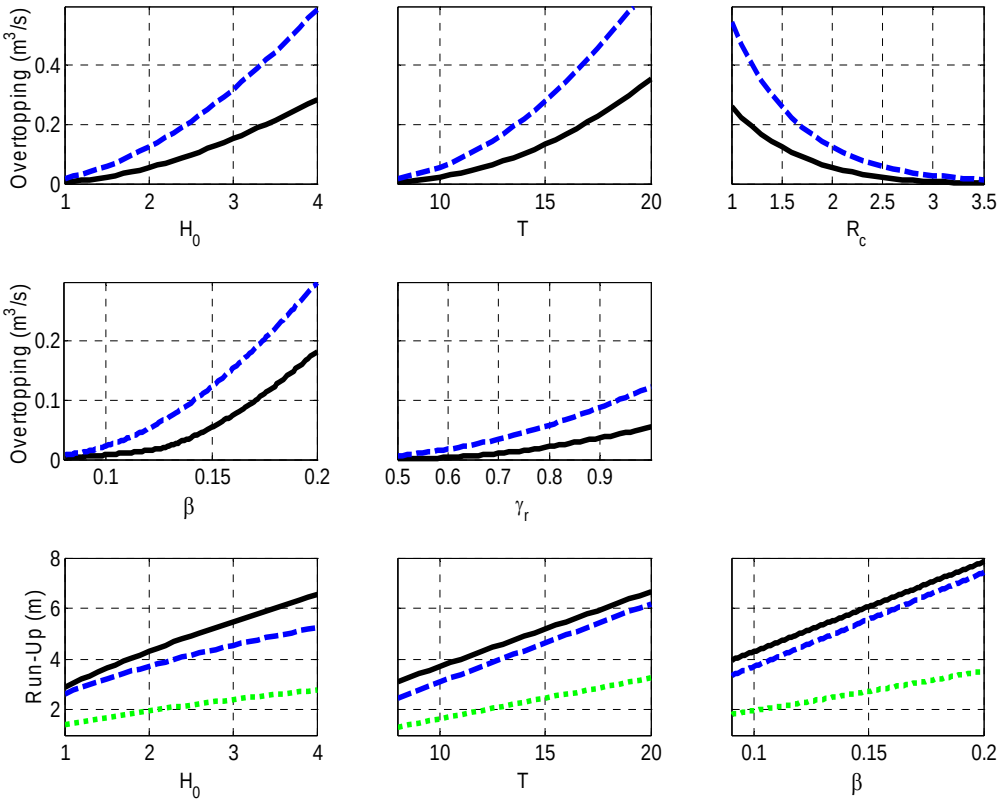

Figure 8. Model sensitivity of the European and HR overtopping models versus the model input parameters (Figures a-e). The run-up models versus the input parameters for the HR, European, and Stockdon run-up models (Figures g-h). The VJ model was not included because the periods used were neither peak nor mean.

Table 1. Cases 1–3 wave, tide, lagoon, and beach parameters. The last column is for Case 3 but with the new peak period of 12.5s. Wave direction in degrees where perpendicular to the shoreline is 0, with north positive and south negative.

Event Date	7-Feb-09	26-Oct-08	20-Sep-06	20-Sep-06
Case	1	2	3	Tp=12.5s
Ocean				
wave height (m)	2.0–3.1	1.5–1.7	1.4–2.2	
peak period range (s)	12.5–13.3	18.2–20	8.3–13.3	
mean period range (s)	8.67–10.65	10.26–14.65	8.33–11.76	
tides (m)	-0.32–2.13	0.30–1.41	0.18–1.68	
H/L	0.015–0.019	0.0048–0.009	0.018–0.019	
H/Lp	0.008–0.012	0.0024–0.003	0.008–0.017	
dir(deg)	-4 – -2	-16 – -15	0 –12	-3 – -1
$\xi(T_p)$	0.79–2.11	1.71–2.84	0.65–2.50	0.89–2.98
$\xi(T_{m0})$	0.63–1.57	1.04–2.00	0.61–1.70	0.61–1.70
Lagoon				
lagoon height chg (m)	0.16	0.08	0.07	
lagoon vol chg (x10^3m)	24.7	7.5	6.1	
Beach				
beach survey date	25-Jan-09	16-Oct-08	12-Sep-06	
slope	0.09–0.19	0.10–0.14	0.08–0.22	
berm height (m)	4.37–6.09	3.66–4.99	4.57–5.82	

Table 2. Reduction factors used to calibrate the models for each case and the consequent r-squared value, slope of the regression, and y-intercept.

Case 1	Reduction Factor	R^2	Slope	y-intercept
HR	1.00	0.76	4.90	2.14
	0.72	0.85	1.00	0.17
European	1.00	0.82	3.00	1.29
	0.79	0.86	1.01	0.30
VJ	1.00	0.75	6.18	3.39
	0.66	0.83	1.00	0.30
Case 2				
HR	1.00	0.64	3.48	0.66
	0.81	0.72	0.99	0.08
European	1.00	0.83	4.00	0.38
	0.75	0.86	0.99	0.04
VJ	1.00	0.78	4.41	0.71
	0.73	0.82	1.00	0.08
Case 3				
HR	1.00	0.08	0.21	0.01
European	1.00	0.16	0.09	0.04
VJ	1.00	0.10	0.56	0.06
Case 3, Tp=12.5				
HR	1.00	0.86	1.59	0.13
	0.94	0.87	1.02	0.06
European	1.00	0.16	0.09	0.04
VJ	1.00	0.83	2.78	0.35
	0.87	0.84	1.03	0.13

APPENDIX B. LIST OF VARIABLES

$R_{2\%}$ The vertical distance above the still water level that a wave travels up a beach face. Run-up height, 2% of waves exceed this value

R_{max} Max run-up height, no waves exceed this value

R_C Freeboard height, distance between the berm height and mean water level

Q Overtopping $\frac{m^3}{s}$ *per m* length of berm

H_S Significant offshore wave height

L_0 Offshore wavelength $= \frac{gT^2}{2\pi}$

T_P Peak period

T_{m0} Mean spectral period

ξ Iribarren number $= \frac{\beta}{\left(\sqrt{H / L_0}\right)}$

ξ_{m0} Iribarren number calculated with mean spectral period

ξ_p Iribarren number calculated with peak period

β Beach slope

g Acceleration of gravity

V Lagoon volume

h Lagoon water level

q River inflow

$\overline{\eta}$ Wave set-up

S_{inc} Incidence swash

S_{IG} Infragravity swash

APPENDIX C. BEACH MORPHOLOGY

Table 3. List of beach surveys conducted at NPS and are in shapefile format.

NPS Beach Surveys	
12-Jan-06	river survey
12-Sep-06	
16-Oct-08	
20-Jan-09	
25-Jan-09	
13-Feb-09	
17-Feb-09	
20-Feb-09	
4-Mar-09	
18-Mar-09	
24-Mar-09	river survey
31-Mar-09	
24-Apr-09	
8-May-09	
18-May-09	

THIS PAGE INTENTIONALLY LEFT BLANK

LIST OF REFERENCES

Allsop, N.H., Hawkes, P.J., Jackson, F.A., Franco, L., 1985. Wave run-up on steep slopes-model tests under random waves. Report No. SR2. Hydraulics Research Ltd, Wallingford.

Baldock, T.E., Weir, F., Hughes, M.G., 2008. Morphodynamic evolution of a coastal lagoon entrance during swash overwash. Geomorphology, 95, 398–411.

Basco, D.R., Shin, C.S., 1999. A one-dimensional numerical model for storm-breaching of barrier islands. J. of Coastal Research 15(1), 241–260.

Battalio, B., Danmeier, D., Williams, P., 2006. Predicting Closure and Breaching Frequencies of Small Tidal Inlets- A Quantified Conceptual Model. Coastal Engineering, 3937–3949.

Battjes, J.A., 1974. Surf Similarity, Proceedings of the 14th Conference of Coastal Engineering. ASCE, 466–480.

Besley, P., 1999. Overtopping of Seawalls: Design and Assessment Manual. Bristol, U.K.: Environment Agency, R&D Technical Report W178, 37.

Bruun, P., 1986. Morphological and navigational aspects of tidal inlets on littoral drift shores. J. Coastal Res. 2(2), 123–145.

Goda, Y., 2009. Derivation of unified wave overtopping formulas for seawalls with smooth, impermeable surfaces based on selected CLASH datasets. Coastal Engineering, 56, 385–399.

Guza, R.T., Thornton, E.B., 1982. Swash oscillations on a natural beach. J. of Geophysical Research, 87(C1), 483–491.

Hedges, T.S., Reis, M.T., 1998. Random wave overtopping of simple sea walls: a new regression model. Proceedings from Institution of Civil Engineers: Water, Maritime and Energy, 130(1), 1–10.

Holland, K.T., Holman, R.A., 1993. The Statistical Distribution of Swash Maxima on Natural Beaches. J. of Geophysical Research, 98(10), 10, 271–10,278.

Hope, A., 2007. RMC Water and Environment, Carmel River Lagoon Hydrographic Survey and Stage-Volume Relationship, prepared for the Monterey Peninsula Water Management District,1–8. Retrieved on August 12, 2009, from http://www.mpwmd.dst.ca.us/Mbay_IRWM/IRWM_library/CarmelBay/CRL-st-vol-TM%2029Nov07.pdf

Hunt, I.A., 1959. Design of seawalls and breakwaters. Journal of Waterways and Harbours Division, ASCE, 85(WW3), 123–152.

James, G., 2009. Personal Communication.

James, G., 2005 Technical Advisory Committee (TAC). Study plan for long term adaptive management of the Carmel River State Beach and Lagoon.

Kraus, N.C., Militello, A., Todoroff, G., 2002. Barrier breaching process and barrier spit breach, Stone Lagoon, California. Shore and Beach, 70(4), 21–28.

Kraus, N.C., 2003. Analytical model of incipient breaching of coastal barriers. Coastal Engineering Journal, 45 (4), 511–531.

Kraus, N.C., 2008. Barrier beach breaching from the lagoon side, with reference to Northern California. Shore and Beach, 76(2), 33–43.

Lanka Hydraulic Institute, 1997. Chilaw achorage flushing study. Interim report, LHI-96-2, Landka Hydraulic Institute, Sri Lanka.

Largier, J.L., Springer, J.H., Talijaard, S., 1992. The stratified hydrodynamics of the Palmiet–a prototype bar-built estuary. In: Prandle, D. (Ed.), Dynamics and Exchanges in Estuaries and the Coastal Zone. American Geophysical Union, 135–154.

Mase, H., Hedges, T.S., Shareef, M., Nagahashi, S., 2003. Wave overtopping formula for gentle slopes incorporating wave runup. Proceedings of Coastal Engineering, JSCE 50, 636–640.

Matias, A., Vila-Concejo, A., Ferreira, O., Morris, B., Dias, J.A., 2009. Sediment Dynamics of Barriers with Frequent Overwash. J. of Coastal Research, 25(3), 768–780.

National Geodetic Survey (NGS) Orthometric height convertion tool. http://www.ngs.noaa.gov/cgi-bin/VERTCON/vert_con.prl (last accessed on 27August 2009).

Owen, M.W., 1980. Design of Seawalls Allowing for Wave Overtopping, Technical Report EX-924. HR-Wallingford, UK.

Pullen, T. Allsop, N.W.H., Bruce, T., Kortenhaus, A., Schuttrumpf, H., van der Meer, J.W., 2007. EurOtop: Wave overtopping of sea defences and related structures: Assessment Manual. Retrieved on August 12, 2009, from www.overtopping-manual.com

Ranasinghe, R., Pattiaratchi, C., 2003. The seasonal closure of tidal inlets: causes and effects, Coastal Engineering J., 45(4), 601–627.

Reeve, D.E., Soliman, A., Lin, P.Z., 2008. Numerical study of combined overflow and wave overtopping over a smooth impermeable seawall. Coastal Engineering, 55, 155–166.

Reis, M.T., Hu, K., Hedges, T.S., Mase, H. A., 2008. Comparison of Empirical, Semiempirical, and Numerical Wave Overtopping Models. J. of Coastal Research, 24, 250–262.

Raubenheimer, B., Guza, R.T., Elgar, S., Kobayashi, N., 1995. Swash on a gently sloping beach. J. of Geophysical Research, 100 (C5), 8751–8760.

Ruggiero, P., Holman, R.A., Beach, R.A., 2004. Wave run-up on a high-energy dissipative beach. J. of Geophysical Research, 109 (C6).

Smith, G.L., Zarillo, G.A., 1988. Short-Term Interactions Between Hydraulics and Morphodynamics of a Small Tidal Inlet, Long Island, New York. J. of Coastal Research, 4(2), 301–314.

Storlazzi, C.D., Field, M.E., 2000. Sediment distribution and transport along a rocky, embayed coast: Monterey Peninsula and Carmel Bay, California. Marine Geology, 170, 289–316.

Stretch, D.D., Parkinson, M.G., 2006. The breaching of sand barriers at perched, temporarily open/closed Estuaries- A model study. Coastal Engineering J. 48 (1), 13–30.

Stockdon, H.F., Holman, R.A., Howd, A.H., Sallenger, A.H., 2006. Coastal Engineering, 53, 573–588.

Tuan, T.Q., Stive, M.J., Verhagen, H.J., Visser, P.J., 2008. Process-based modeling of the overflow-induced growth of erosional channels. Coastal Engineering, 55, 468–483.

Van der Meer, J.W., Janssen, W., 1995. Wave run-up and wave overtopping at dikes. In: Kabayashi, Demirbilek (Eds.), Wave Forces on Inclined and Vertical Wall Structures. American Society of Civil Engineers, New York: ASCE, 1–27.

Visser, P.J., 1998. Proc. 26th Coastal Eng. Conf., ASCE: Breach erosion of sand dikes, 3516–3528.

Watson, F.R., Casagrande, J., 2004. Potential Effects of Groundwater Extractions on Carmel Lagoon, California. The Watershed Institute, California State University Monterey Bay, Report No. WI–2004–09.

INITIAL DISTRIBUTION LIST

1. Defense Technical Information Center
   Ft. Belvoir, Virginia

2. Dudley Knox Library
   Naval Postgraduate School
   Monterey, California

3. Professor Jamie MacMahan
   Naval Postgraduate School
   Monterey, California

4. Professor Jeffrey Paduan
   Naval Postgraduate School
   Monterey, California

5. Larry Hampson
   Monterey, California

6. Professor Edward Thornton
   Naval Postgraduate School
   Monterey, California